Bulk effects on topological conduction in three-dimensional topological insulators

Quansheng Wu
Institute of Applied Physics and Computational Mathematics, Beijing 100094, China
and CAEP Software Center for High Performance Numerical Simulation, Beijing 100088, China

Vincent E. Sacksteder IV*
Institute of Physics, Chinese Academy of Sciences, Beijing 100190, China
and Division of Physics and Applied Physics, Nanyang Technological University, 21 Nanyang Link, Singapore 637371
(Received 26 September 2013; revised manuscript received 29 May 2014; published 14 July 2014)

The surface states of a topological insulator in a fine-tuned magnetic field are ideal candidates for realizing a topological metal which is protected against disorder. Its signatures are (i) a conductance plateau in long wires in a finely tuned longitudinal magnetic field and (ii) a conductivity which always increases with sample size, and both are independent of disorder strength. We numerically study how these experimental transport signatures are affected by bulk physics in the interior of the topological insulator sample. We show that both signatures of the topological metal are robust against bulk effects. However the bulk does substantially accelerate the metal's decay in a magnetic field and alter its response to surface disorder. When the disorder strength is tuned to resonance with the bulk band the conductivity follows the predictions of scaling theory, indicating that conduction is diffusive. At other disorder strengths the bulk reduces the effects of surface disorder and scaling theory is systematically violated, signaling that conduction is not fully diffusive. These effects will change the magnitude of the surface conductivity and the magnetoconductivity.

DOI: 10.1103/PhysRevB.90.045408 PACS number(s): 73.25.+i, 71.70.Ej, 73.20.Fz, 73.23.−b

I. INTRODUCTION

The Dirac fermions residing on the surface of strong topological insulators (TIs) provide a new opportunity for realizing a topological metal which remains conducting regardless of disorder strength or sample size [1–7]. This metal should be general to any single species of Dirac fermions which breaks spin symmetry but retains time-reversal symmetry. When the Fermi level is tuned inside the TI's bulk band gap, all states inside the TI bulk are localized. Conduction can occur only on the TI surface, which hosts a single species of two-dimensional (2D) Dirac fermions.[1] These are predicted to remain always conducting regardless of disorder strength, forming a topological metal.

Many beautiful TI experiments have visualized the Dirac cone, spin-momentum locking, Landau levels with $\sqrt{n}$ spacing, and SdH oscillations [8,9]. These signals are visible only when either momentum or the Landau level index are approximately conserved; they disappear when disorder is strong. In contrast, the topological metal's hallmark is robust surface conduction at any disorder strength and in large samples, even when disorder destroys the Dirac cone. In this article we will focus on experimental signatures of this protection against disorder.

We will show that bulk physics in the TI's interior substantially modifies the topological metal. Even though it is a surface state, in response to disorder it may explore the TI bulk or even tunnel between surfaces. We used several months on a large parallel supercomputer to perform extensive calculations of conduction, including both bulk and surface physics.

Two experimental signatures are available for proving incontrovertibly that a topological metal is indeed robust against disorder. The first is a quantized conductance in long wires. In ordinary wires the conductance G decreases with wire length until only one channel remains open, i.e. $G = \frac{e^2}{h}$ and then transits into a localized phase where the last channel decays exponentially. In contrast the topological metal exhibits one *perfectly conducting channel* (PCC) which remains forever topologically protected, so in long wires the conductance is quantized at $G = \frac{e^2}{h}$ [10–17]. The PCC can be realized only when there is no gap in the surface states' Dirac cone. In TI wires locking between spin and momentum creates a gap, but a specially tuned longitudinal magnetic field B can be used to close the gap and realize the PCC's quantized conductance. In this fine-tuned scenario B breaks time-reversal symmetry and causes the PCC to eventually decay. Our results will confirm the PCC's robustness against bulk effects, and show that both the optimal value of B and the PCC's optimal decay length are altered by bulk physics. These results, and the PCC's response to sample dimensions, magnetic fields, and disorder, will be useful to experimental PCC hunters.

The second key signature of the topological metal concerns the diffusive regime, where the sample aspect ratio L/W is small enough that several conducting channels remain open, but the sample is still bigger than the scattering length. (W and L are the sample width and length.)

In this regime, regardless of disorder strength, a topological metal's *conductivity* $\sigma = GL/W$ *always increases when the length* L *and width* W *are increased in proportion to each other* [18–26]. This signature contrasts with nontopological materials where the conductivity can always be forced to decrease by making the disorder large enough [19,27]. In both cases the increasing conductivity—called weak antilocalization (WAL)—can be removed by introducing a weak magnetic

*vincent@sacksteder.com
[1]More generally, any odd number of fermions is possible.

field; experimental studies of the TI magnetoconductivity are extremely popular. In the diffusive regime both the conductivity and the magnetoconductivity are expected to follow universal curves prescribed by scaling theory, independent of sample details.

Here we will confirm that the always-increasing conductivity is robust against both bulk effects and very strong disorder. We will also show that the bulk reduces scattering and causes violation of the universality predicted by scaling theory, which suggests that the topological metal's conduction is not purely diffusive. This has immediate consequences for experiments: we expect that magnetoconductivity measurements are sensitive to bulk physics, and that the magnitude of the observed signal will vary systematically with the Fermi level and disorder strength.

Lastly, we find that the bulk reduces the effects of scatterers residing on the TI surface. The topological metal is free to reroute around scatterers, into the TI bulk. This is a second level of topological protection, in addition to the well-known suppression of backscattering. It should change the surface conductivity and increase the topological metal's robustness against issues of sample purity, substrates, gating, etc.

II. MODEL

The topological metal is independent of any short-scale variation in the TI sample, including any microscopic details of the Hamiltonian. Its two signatures are regulated by only two parameters: the scattering length and localization length. Because we are concerned with Fermi energies inside the bulk band gap, bulk effects on the topological metal can depend on only a small number of parameters—the Fermi level, the Fermi velocity, the penetration depth, the bulk band gap, and the bulk spectral width. Therefore we study a computationally efficient minimal tight-binding model of a strong TI implemented on a cubic lattice with dimensions H, W, and L. With four orbitals per site, the model's momentum representation is

$$\mathcal{H}(\vec{k}) = 2\Gamma^1 - \frac{1}{2}\sum_{i=1}^{3}(\Gamma^1 - \imath\Gamma^{i+1})e^{-\imath k_i a} + \text{H.c.} \qquad (1)$$

Γ^i are the Dirac matrices $1\otimes\sigma_z, -\sigma_y\otimes\sigma_x, \sigma_x\otimes\sigma_x, -1\otimes\sigma_y$, $a = 1$ is the lattice spacing, and the penetration depth is $d \propto a$ [28]. We include a magnetic field oriented longitudinally along the axis of conduction by multiplying the hopping terms by Peierls phases.[2] This noninteracting model exhibits a spectral width $\Delta E = 10$, a bulk band gap in the interval $E = [-1,1]$, a single Dirac cone in the bulk gap, and Fermi velocity $v_F = 2$. To this model we add uncorrelated white noise disorder $u(x)$. On each individual site the disorder is proportional to the identity and its strength is chosen randomly from the interval $[-U/2, U/2]$, where U is the disorder strength. We attach two clean semi-infinite leads that have $W \times H$ cross-sections equal to that of the sample itself and evaluate the conductance using the Caroli formula [29,30] $G = -\frac{e^2}{h}\text{Tr}((\Sigma_L^r - \Sigma_L^a)G_{LR}^r(\Sigma_R^r - \Sigma_R^a)G_{RL}^a)$. $G^a, G^r = (E_F - \mathcal{H} - u \mp \imath\epsilon)^{-1}$ are the advanced and retarded single-particle Green's functions connecting the left and right leads, and $\Sigma_{L,R}$ are the lead self-energies [31].

In our study we will leave the TI bulk pure, since the main effects of bulk disorder on the surface states can be duplicated by adjusting the bulk parameters. In particular, the bulk band width widens, the bulk band gap narrows, and the penetration depth increases. These parameters are only weakly sensitive to disorder when the disorder is small compared to the band width. When the disorder strength approaches the band width the bulk states gradually delocalize, surface states are eventually destroyed by tunneling through the bulk, and the material ceases to be a TI [32–36]. In contrast our focus here is on bulk effects on a healthy topological metal, which are controlled only by the few bulk parameters that we have listed.

We include only surface disorder, which has been extensively investigated experimentally because practical TI devices may be capped, gated, bombarded, or left exposed to atmosphere [37–46].

III. PERFECTLY CONDUCTING CHANNEL

In Figs. 1 and 2 we focus on the topological metal's PCC signature, which is a quantized conductance plateau seen in very long samples. We set the disorder strength to $U = 2$, and the Fermi energy is $E_F = 0.7$ in both the sample and the leads. Figure 1(a) shows the plateau in $W \times H$ slabs, which retain all bulk physics but are simplified by avoiding the gap in the surface Dirac cone. The plateau conductance is $G = 2\frac{e^2}{h}$ because each surface hosts a PCC. We define the PCC decay length λ, i.e. the plateau length, as the wire length where the

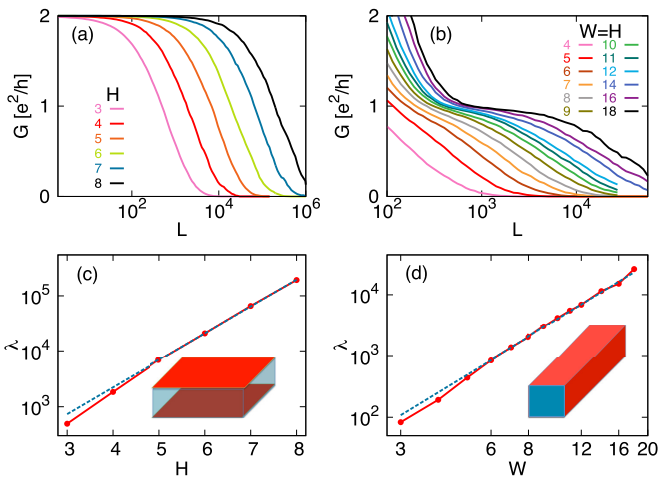

FIG. 1. (Color online) The perfectly conducting channel (PCC), a topologically protected conductance plateau in very long TI samples. (a), (b) The conductance plateau as a function of length L in (a) $W \times H$ slabs with no magnetic field, and in (b) $W \times W$ wires with a fine-tuned longitudinal field. (c) In slabs the decay length λ is controlled by tunneling and scales exponentially with slab height H. (d) In wires the decay length scales with W^3 and is caused by the surface state's penetration into the bulk. The dotted lines are (c) $\lambda \propto \exp(1.12\ H)$ and (d) $\lambda = 4W^3$.

[2]We neglect the Zeeman term. This term will be small and proportional to $1/W^2$ because the PCC conductance plateau occurs at a value of B, which is proportional to $1/W^2$.

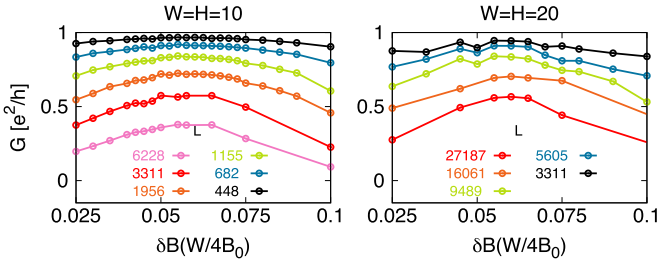

FIG. 2. (Color online) The conductance plateau's dependence on magnetic field B at disorder strength $U = 2$. The wire lengths of the 20×20 wires (right) are chosen to be about eight times bigger than the wire lengths of the 10×10 wires (left). On the x axis we plot the magnetic field, rescaled by $W/4B_0 \propto W^3$. The match between the 10×10 and 20×20 wires proves that the decay length scales with W^3 and that the conductance peak's width (in B) scales with W^{-3}. At $U = 2$ bulk effects cause the conductance peak to shift to a larger field strength, so we have subtracted from B the optimal field strength B_0 at zero disorder.

conductance is half of its plateau value.[3] Figure 1(c) shows that λ grows exponentially as the slab height H increases from 3 to 8, which proves that the PCC decay is caused by tunneling and is exponentially small except in very thin slabs [47]. This is disorder-enabled tunneling; λ diverges in pure slabs.

Next we turn to $W \times W$ TI wires, where the PCC is realized only after we remove the gap in the Dirac cone. Since spin is locked to momentum in TIs, parallel transport of the spin on one circuit around a wire's circumference causes a π Berry phase. This causes a small gap $\Delta_B = 2\sqrt{2}v_F/C$ where C is the wire circumference. However the π phase can be canceled and the gap removed if the magnetic flux through the wire is fine tuned to produce an additional π phase [15,16,49–51]. Figure 1(b) shows our results after numerically optimizing B to maximize the PCC lifetime, which at leading order kept the magnetic length $L_B \propto \sqrt{\hbar/eB}$ proportional to the wire width W. The obvious PCC conductance plateau confirms that the topological metal is robust in wires.

Figure 1(d) presents the first numerical calculations of the PCC decay length λ's dependence on the wire width W in a model that includes the TI bulk. Our results are of high accuracy, with errors of a few percent. They required calculation of very long and wide wires, numerical optimization of B, and many samples (from $N = 864$ for $W \leqslant 12$ to $N = 80$ for $W = 18$). They prove that PCC decay in wires is much faster than a slab's exponentially slow decay, and that λ scales with the cube of the wire width $\lambda \approx \alpha W^3$, with prefactor $\alpha \approx 4$. This points to the magnetic field and not tunneling as the dominant source of PCC decay in TI wires.

The decay length's cubic W^3 scaling is caused by bulk physics. Previously $\lambda \propto W^4$ scaling was predicted based on a bulk-independent mechanism [16,52]. Diffusion into the bulk [53] is also expected to scale with $L_B^4 \propto W^4$. If we note that the large value of α prohibits instances of the inverse scattering length $l^{-1} \approx 1/30a$ [48], then simple dimensional analysis obtains $\lambda \propto W^3/d^2$, where $d \propto a$ is the penetration depth of the surface states. This implies that the fastest mechanism of PCC decay is caused by the surface state's penetration into the bulk.

Bulk physics also combines with surface disorder to alter the magnetic field strength, which maximizes λ. In any TI disorder on the surface will push the topological states into the bulk, rescaling their magnetic cross section by $(1 - 4\delta/W)$ [28,47,54]. δ is their displacement, which can be determined from the shift in optimal magnetic field via $\delta = (B_{opt} - B_0)(W/4B_0)$, where B_{opt} and B_0 are respectively the optimal fields at finite disorder U and at zero disorder $U = 0$. Figure 2 plots the conductance at $U = 2$ as a function of $\delta B\,(W/4B_0)$, $\delta B = B - B_0$. It shows that the displacement at $U = 2$ is about 0.06 lattice units and the change in optimal field is $B_{opt} - B_0 = 0.24\,B_0/W$.

Figure 2 shows that after rescaling by $W/4B_0$ the conductance peak has the same position and width in both 10×10 and 20×20 wires. This proves that both the optimal value and the peak width of the magnetic field scale with $B_0\delta/W \propto W^{-3}$. In thick wires the PCC will not be visible unless the magnetic field is very finely tuned with an accuracy proportional to W^{-3}. We expect that this formula, the previous scaling formulas, and the graphs of the PCC peak will all be useful for PCC hunters.

IV. CONDUCTIVITY

In Fig. 3 we turn to studying the topological metal's second signature, a conductivity σ, which grows robustly with sample size regardless of disorder strength. We have carefully controlled for many effects and errors. σ grows only in the diffusive regime where several channels remain conducting, and here it is independent of sample width W. Figure 3(a) shows that both σ and its logarithmic derivative $\beta(L) = d\ln\sigma/d\ln L$ converge to their diffusive values when $W > 1.1\,L$; we restrict our remaining data to this converged regime. Moreover in the diffusive regime both large slabs and large wires have the same conductivity; the gap is erased by disorder, and has no effect even at $E = 0$ [48]. Here we report results obtained from slabs. We also ensure convergence with slab height H by using thick slabs with $H = 6$ in Fig. 3(a) and $H = 12$ elsewhere. The associated computational cost is compounded by β's sensitivity to statistical errors; very large $N = 960$–4800 numbers of samples—and smoothing in Figs. 3(a) and 3(c)—were necessary to obtain these low-noise β curves. Leads effects are minimized by doping them into the metallic bulk band at $E_F = 2$.

The most prominent feature of our data is highlighted in Fig. 3(c): a resonance between the disordered surface states and the bulk band, seen here as a valley in both $2/\pi\sigma$ and β, which we have plotted as functions of disorder U at four Fermi levels inside the gap. It is centered around disorder strength $U = [6,10]$, matching the bulk band width $\Delta E = 10$. The resonance is generic to all TIs, since its physics is generic: surface disorder displaces the surface states into the bulk, as we already saw in Fig. 2. At weak disorder U the displacement is small ($\delta = 0.06$ at $U = 2$ in our model), but as U passes through the resonance center the surface states migrate from

[3]The Supplemental Material [48] shows that in slabs λ is roughly independent of the slab width W, and that $W = 3$ gives results that are quite close to the converged value. In Fig. 1 we use narrow $W = 3$ slabs, allowing calculation of very long wires.

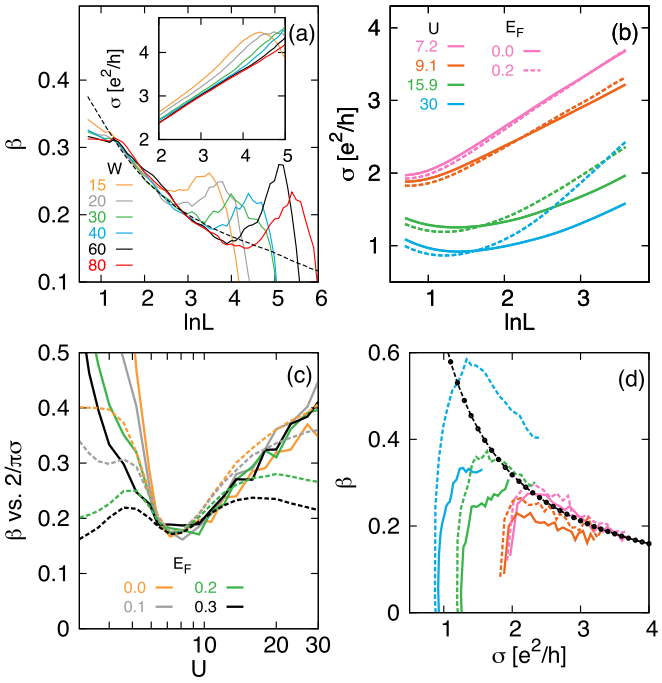

FIG. 3. (Color online) The conductivity σ and its logarithmic derivative $\beta(L) = d\ln\sigma/d\ln L$. (a) Convergence of β and σ (in inset) as the sample width W is increased from 15 to 80. (c) The resonance between the topological surface state and the bulk band, manifested as valleys in both β (solid lines) and $2/\pi\sigma$ (dashed lines). At the resonance center the topological state is most strongly disordered, and also exhibits the largest conductivity. (b) Topological protection ensures that the surface states' conductivity σ always increases with sample size L, as verified here near the resonance center $U = 7.2$, off center $U = 9.1$, and in the large-disorder shoulder $U = 15.9,30.0$. At very small L tunneling through the bulk causes σ to decrease with L. The variation in line slope with U and with Fermi energy E_F breaks the universality predicted by scaling theory. (d) The β function. Scaling theory predicts a universal $\beta = 2/\pi\sigma$ curve independent of U and E_F, shown here as a black dotted-dashed curve, and also shown in (a). The deviations from universality seen here imply similar behavior in the magnetoconductivity.

the disordered surface layer into the clean bulk. At the resonance center scattering is maximized, as is mixing between the bulk and the surface states. Since quantum scattering processes are responsible for the conductivity's growth, σ is also maximized at the resonance center. We conclude that outside the resonance center the bulk tends to decrease the effect of surface disorder. This will change the magnitude of the surface conduction in TI samples and will also change the scattering length and the diffusion constant, each of which can be observed experimentally.

Figure 3(c) shows a very interesting feature: at the resonance center the four conductivity curves kiss, which signals that scattering is independent of energy. The surface density of states (DOS) ρ also must be independent of energy, since it determines the scattering time via $\tau \propto (\langle U^2\rangle\,\rho)^{-1}$. This is in remarkable contrast with the linear DOS $\rho(E) \propto E$ seen at zero disorder.

Figure 3(b) examines the the conductivity growth signature of topological metals at two values of the Fermi level $E_F = 0, 0.2$ and four representative disorder strengths. The growth is very clear in the two pink lines at the top, which lie near the resonance center $U = 7.2$, and also in the slightly lower two orange lines, which lie slightly off center $U = 9.1$. The lowest four lines lying in the resonance shoulder $U = 15.9, 30.0$ do reveal a decreasing conductivity at small L, but this is a finite-size effect from the leads: disorder-assisted bulk tunneling between the leads increases σ in very short samples, and this excess decreases rapidly with L [48]. Leaving aside this tunneling effect, we find that σ grows even when its value (per surface) is as small as $\sigma \geqslant 0.31\frac{e^2}{h} \approx \frac{1}{\pi}\frac{e^2}{h}$. This contrasts with materials without topological protection where any value of σ up to $\sigma_C \approx 1.4\frac{e^2}{h}$ produces a decreasing conductivity [19,27,55–58], and proves that a TI's conductivity growth is robust against bulk effects.

The details of Fig. 3 can be compared with the one parameter scaling theory of conduction, which makes specific predictions about the diffusive regime. Scaling theory's most important prediction is universality: the only effect of changing the disorder strength and Fermi level should be to rescale both the scattering length l and the overall length scale [59]. The β function is not sensitive to l, so it should be universal. Numerical works on topological metals have shown that this universal curve agrees quite well with $\beta(\sigma) = 1/\pi\sigma$, even when $\sigma \approx 1/\pi$ is quite small [19,20,25,60]. In consequence σ grows logarithmically $\propto 1/\pi\ \ln L$. In our TI slabs β and σ are multiplied by 2 for the two surfaces. In summary, scaling theory predicts that in Fig. 3(d) the $\beta(\sigma)$ curves should all coincide with each other and with the $2/\pi\sigma$ black dotted line, and that in Fig. 3(c) each solid $\beta(\sigma)$ line should coincide with its partnering dashed $2/\pi\sigma$ line. Moreover the conductivity curves in Fig. 3(b) should all follow straight lines with the same slope $2/\pi$. These universal results are at the origin of the Hikami-Larkin-Nagaoka formula which gives a universal prediction for the conductivity's response to a small magnetic field, and in particular the $2/\pi$ coefficient in these scaling theory predictions transfers over directly to the HLN formula's magnitude [60].

Near the resonance center $U \approx 7.2$ we find excellent agreement with scaling theory, as evidenced by the pink straight line conductivity curves found in Fig. 3(b) and by the pink β curves in Fig. 3(d), which coincide nicely with $2/\pi\sigma$. The excellent agreement with scaling theory indicates that at the resonance center conduction is completely determined by diffusion and its quantum corrections, and that the scattering length is very small.

At other disorder strengths we find that scaling theory's universality is systematically violated. We begin well within the resonance at $U = 9.1$, which is shown in the orange lines in Figs. 3(b), 3(d). These lines are straight, indicating that the conductivity grows with the dimensionless quantity $\ln L$, and proving that σ is not controlled by any finite-size effect. However the lines' slopes are clearly smaller than the $U = 7.2$ slope (20% smaller at $E = 0$ and 12% at $E = 0.2$), so β is smaller than scaling theory's $2/\pi\sigma$. Figure 3(c) confirms this, showing that at disorder strengths near the resonance center the solid β lines lie consistently below the dashed $2/\pi\sigma$ lines. This cannot be attributed to finite-size effects or other errors, and is an unambiguous signal of nonuniversality.

Turning to the resonance shoulder ($U = 15.9, 30.0$), at large L we find that β consistently exceeds the universal scaling theory prediction $2/\pi\sigma$ for $E = 0.2,0.3$, as seen both in Fig. 3(c) and in the blue dotted $E = 0.2, W = 30$ curves in Figs. 3(b), 3(d). This nonuniversal conduction is likely superdiffusive, somewhere between diffusion and ballistic motion. Once again this cannot be a finite-size effect, since Fig. 3(b) shows that in long $L = 35$ samples σ always becomes roughly linear, i.e. proportional to $\ln L$. This is confirmed by Fig. 3(d), which shows β converging toward the decreasing $\beta \propto 1/\sigma$ form, which accompanies $\sigma \propto \ln L$. We have checked that in longer $L \leqslant 70$ samples all of the β curves shown here begin decreasing.

We conclude that the TI bulk reduces the topological metal's scattering and leaves the conductivity in a nondiffusive, nonuniversal regime that is sensitive to sample details such as disorder strength and Fermi level. This has immediate consequences for experimental measurements of the magnetoconductivity. In particular, its magnitude should be sensitive to variations of the disorder strength and the Fermi level, in synchrony with the changing magnitude of β and σ.

V. CONCLUSIONS

In summary, our results confirm that the topological metal is robust against bulk effects when a finely tuned magnetic field is applied, but also reveal that its response to disorder and to the magnetic field is substantially changed by the bulk. The bulk alters the PCC's decay, protects the topological metal from surface disorder except when the disorder is in resonance with the bulk, and pushes conduction into a nondiffusive, nonuniversal regime where it is sensitive to the Fermi energy and the disorder strength.

ACKNOWLEDGMENTS

We acknowledge useful discussions with T. Ohtsuki, K. Kobayashi, B. A. Bernevig, D. Culcer, and A. Petrovic, and thank the Zhejiang Institute of Modern Physics and Xin Wan for hosting a workshop, which allowed fruitful discussions. This work was supported by the National Science Foundation of China and by the 973 program of China under Contract No. 2011CBA00108. We thank Xi Dai and the IOP, who hosted and supported this work.

[1] C. L. Kane and E. J. Mele, Phys. Rev. Lett. **95**, 226801 (2005).
[2] H. Min, J. E. Hill, N. A. Sinitsyn, B. R. Sahu, L. Kleinman, and A. H. MacDonald, Phys. Rev. B **74**, 165310 (2006).
[3] H. Zhang, C.-X. Liu, X.-L. Qi, X. Dai, Z. Fang, and S.-C. Zhang, Nat. Phys. **5**, 438 (2009).
[4] M. Z. Hasan and C. L. Kane, Rev. Mod. Phys. **82**, 3045 (2010).
[5] Y. Q. Li, K. H. Wu, J. R. Shi, and X. C. Xie, Front. Phys. **7**, 165 (2012).
[6] D. Culcer, Physica E **44**, 860 (2012).
[7] J. H. Bardarson and J. E. Moore, Rep. Prog. Phys. **76**, 056501 (2013).
[8] D. Hsieh, D. Qian, L. Wray, Y. Xia, Y. S. Hor, R. J. Cava, and M. Z. Hasan, Nature (London) **452**, 970 (2008).
[9] T. Hanaguri, K. Igarashi, M. Kawamura, H. Takagi, and T. Sasagawa, Phys. Rev. B **82**, 081305(R) (2010).
[10] M. R. Zirnbauer, Phys. Rev. Lett. **69**, 1584 (1992).
[11] A. D. Mirlin, A. Muller-Groeling, and M. R. Zirnbauer, Ann. Phys. (NY) **236**, 325 (1994).
[12] T. Ando and H. Suzuura, J. Phys. Soc. Jpn. **71**, 2753 (2002).
[13] Y. Takane, J. Phys. Soc. Jpn. **73**, 1430 (2004).
[14] S. Ryu, C. Mudry, H. Obuse, and A. Furusaki, Phys. Rev. Lett. **99**, 116601 (2007).
[15] P. M. Ostrovsky, I. V. Gornyi, and A. D. Mirlin, Phys. Rev. Lett. **105**, 036803 (2010).
[16] Y. Zhang and A. Vishwanath, Phys. Rev. Lett. **105**, 206601 (2010).
[17] S. S. Hong, Y. Zhang, J. J. Cha, X.-L. Qi, and Y. Cui, arXiv:1303.1601v1.
[18] P. M. Ostrovsky, I. V. Gornyi, and A. D. Mirlin, Phys. Rev. Lett. **98**, 256801 (2007).
[19] K. Nomura, M. Koshino, and S. Ryu, Phys. Rev. Lett. **99**, 146806 (2007).
[20] J. H. Bardarson, J. Tworzydlo, P. W. Brouwer, and C. W. J. Beenakker, Phys. Rev. Lett. **99**, 106801 (2007).
[21] P. San-Jose, E. Prada, and D. S. Golubev, Phys. Rev. B **76**, 195445 (2007).
[22] J. Tworzydlo, C. W. Groth, and C. W. J. Beenakker, Phys. Rev. B **78**, 235438 (2008).
[23] C. H. Lewenkopf, E. R. Mucciolo, and A. H. Castro Neto, Phys. Rev. B **77**, 081410(R) (2008).
[24] S. Adam, P. W. Brouwer, and S. Das Sarma, Phys. Rev. B **79**, 201404(R) (2009).
[25] E. R. Mucciolo and C. H. Lewenkopf, J. Phys.: Condens. Matter **22**, 273201 (2010).
[26] R. S. K. Mong, J. H. Bardarson, and J. E. Moore, Phys. Rev. Lett. **108**, 076804 (2012).
[27] Y. Asada, K. Slevin, and T. Ohtsuki, Phys. Rev. B **70**, 035115 (2004).
[28] G. Schubert, H. Fehske, L. Fritz, and M. Vojta, Phys. Rev. B **85**, 201105 (2012).
[29] C. Caroli, R. Combescot, P. Nozieres, and D. Saint-James, J. Phys. C **4**, 916 (1971).
[30] Y. Meir and N. S. Wingreen, Phys. Rev. Lett. **68**, 2512 (1992).
[31] M. P. L. Sancho, J. M. L. Sancho, and J. Rubio, J. Phys. F: Metal Physics **15**, 851 (1985).
[32] C. W. Groth, M. Wimmer, A. R. Akhmerov, J. Tworzydlo, and C. W. J. Beenakker, Phys. Rev. Lett. **103**, 196805 (2009).
[33] H.-M. Guo, G. Rosenberg, G. Refael, and M. Franz, Phys. Rev. Lett. **105**, 216601 (2010).
[34] L. Chen, Q. Liu, X. Lin, X. Zhang, and X. Jiang, New J. Phys. **14**, 043028 (2012).
[35] D. Xu, J. Qi, J. Liu, V. Sacksteder, X. C. Xie, and H. Jiang, Phys. Rev. B **85**, 195140 (2012).
[36] K. Kobayashi, T. Ohtsuki, K. I. Imura, and I. F. Herbut, Phys. Rev. Lett. **112**, 016402 (2014).
[37] J. G. Analytis, J.-H. Chu, Y. Chen, F. Corredor, R. D. McDonald, Z. X. Shen, and I. R. Fisher, Phys. Rev. B **81**, 205407 (2010).
[38] M. Brahlek, Y. S. Kim, N. Bansal, E. Edrey, and S. Oh, Appl. Phys. Lett. **99**, 012109 (2011).

[39] R. Valdes Aguilar, A. V. Stier, W. Liu, L. S. Bilbro, D. K. George, N. Bansal, L. Wu, J. Cerne, A. G. Markelz, S. Oh *et al.*, Phys. Rev. Lett. **108**, 087403 (2012).

[40] O. E. Tereshchenko, K. A. Kokh, V. V. Atuchin, K. N. Romanyuk, S. V. Makarenko, V. A. Golyashov, A. S. Kozhukhov, I. P. Prosvirin, and A. A. Shklyaev, JETP Lett. **94**, 465 (2011).

[41] D. Hsieh, Y. Xia, D. Qian, L. Wray, J. H. Dil, F. Meier, J. Osterwalder, L. Patthey, J. G. Checkelsky, N. P. Ong *et al.*, Nature (London) **460**, 1101 (2009).

[42] H. J. Noh, J. Jeong, E. J. Cho, H. K. Lee, and H. D. Kim, Europhys. Lett. **96**, 47002 (2011).

[43] Z. K. Liu, Y. L. Chen, J. G. Analytis, S. K. Mo, D. H. Lu, R. G. Moore, I. R. Fisher, Z. Hussain, and Z. X. Shen, Physica E **44**, 891 (2012).

[44] M. Lang, L. He, F. Xiu, X. Yu, J. Tang, Y. Wang, X. Kou, W. Jiang, A. V. Fedorov, and K. L. Wang, ACS Nano **6**, 295 (2011).

[45] J. Chen, H. J. Qin, F. Yang, J. Liu, T. Guan, F. M. Qu, G. H. Zhang, J. R. Shi, X. C. Xie, C. L. Yang *et al.*, Phys. Rev. Lett. **105**, 176602 (2010).

[46] D. Kong, J. J. Cha, K. Lai, H. Peng, J. G. Analytis, S. Meister, Y. Chen, H.-J. Zhang, I. R. Fisher, Z.-X. Shen *et al.*, ACS Nano **5**, 4698 (2011).

[47] Q. Wu, L. Du, and V. E. Sacksteder, Phys. Rev. B **88**, 045429 (2013).

[48] See Supplemental Material at http://link.aps.org/supplemental/10.1103/PhysRevB.90.045408 for further information on tunneling between leads, finite size effects, and convergence. Also find a comparison of wires with slabs, our calculation of the scattering length, and further comparison with scaling theory.

[49] G. Rosenberg, H.-M. Guo, and M. Franz, Phys. Rev. B **82**, 041104 (2010).

[50] R. Egger, A. Zazunov, and A. L. Yeyati, Phys. Rev. Lett. **105**, 136403 (2010).

[51] J. H. Bardarson, P. W. Brouwer, and J. E. Moore, Phys. Rev. Lett. **105**, 156803 (2010).

[52] T. Ando, J. Phys. Soc. Jpn. **75**, 054701 (2006).

[53] B. L. Altshuler and A. G. Aronov, JETP Lett. **33**, 499 (1981).

[54] J. Dufouleur, L. Veyrat, A. Teichgraber, S. Neuhaus, C. Nowka, S. Hampel, J. Cayssol, J. Schumann, B. Eichler, O. G. Schmidt *et al.*, Phys. Rev. Lett. **110**, 186806 (2013).

[55] T. Kawarabayashi and T. Ohtsuki, Phys. Rev. B **53**, 6975 (1996).

[56] A. Kawabata, in *Lecture Notes in Physics* (Springer-Verlag, Berlin, Heidelberg, 2003), pp. 41–51.

[57] Y. Asada, K. Slevin, and T. Ohtsuki, Physica E **34**, 228 (2006).

[58] P. Markos and L. Schweitzer, J. Phys. A: Math. Gen. **39**, 3221 (2006).

[59] E. Abrahams, P. W. Anderson, D. C. Licciardello, and T. V. Ramakrishnan, Phys. Rev. Lett. **42**, 673 (1979).

[60] S. Hikami, A. I. Larkin, and Y. Nagaoka, Prog. Theor. Phys. Prog. Lett. **63**, 707 (1980).